Detection of motion direction of targets using a turtle retinal patch model

Mervyn P. B. Ekanayake
Department of Electrical and
Electronics Engineering
Univ. of Peradeniya
Sri Lanka

Bijoy K. Ghosh
Department of Mathematics
and Statistics
Texas Tech University
Lubbock, TX 79409, USA

1 Introduction

Direction selectivity is an important feature of visual systems that has caught the attention of neuroscientists for over 100 years [8]. Directionally selective responses have been recorded by Hubel [10] in the primary visual cortex of an awake cat. Subsequently, Barlow and Levick [3] studied direction selectivity in the retinal ganglion cells of rabbits. Our interest in this paper is to study direction selectivity as a part of our ongoing study of modeling the visual pathway of freshwater turtles. In [16], we show that visual inputs produce waves that propagate across the visual cortex of freshwater turtles and visual information is encoded in the cortical waves. In all of our prior models the visual input was directly incident on the lateral geniculate, completely bypassing the retina. The purpose of this paper is to add a model of the retinal cell to the pathway and to study how retinal signals encode a moving point target incident on a small retinal patch. The target is moving with a constant, possibly unknown, velocity along directions that are spread across the entire 360°.

Turtle Retinal ganglion cells are either ON type, OFF type or ON-OFF type. The ON type cells have an excitatory center and inhibitory surrounding. The OFF type cells have an inhibitory center and excitatory surrounding. Finally the ON-OFF type cells have an excitatory center, an inhibitory annulus followed by an outermost excitatory surrounding (e.g. see [15]). Some of the turtle retinal cells are sensitive to the direction of the optical flow of an image sequence, (e.g. [1, 4]). These cells are called, *direction sensitive cells* or the B cells. The other cells, which are not sensitive to the direction of motion (but are sensitive to the intensity of the target), are called the A cells. The A cells can be ON or OFF type, whereas, the B cells are ON-OFF type. The A cells have a larger cell body (soma size) as well as a larger dendritic arborization. This results in a larger receptor field, compared to the B cells (see [15]). The A cells are smaller in number compared to the B cells on the turtle retina [18].

The turtle retina effectively encodes the motion parameters of moving targets in its visual space (see [19]). The retinal ganglion cells encode input signals using a sequence of spikes. We reproduce the spike generation process using a set of filters which model layers of rods and cones in the retina. The A cells have a similar block diagram except the directional filters are absent. The output of the filters are incident on a single compartment spike generating neuronal cell, with primarily sodium and potassium channels, modeled using Hodgkin-Huxley equations (see [9]). For a physiologically detailed model of a single cell that includes many additional channels

(such as transient AHP channel, sustained calcium channel, calcium dependent potassium channel and transient calcium channel), see [7].

We consider a patch of the retina (see Fig. 1a) and circular targets that are moving with unknown constant speed and motion direction (see Fig. 1b). Our objective is described in the following two problems. In the first problem we consider targets that are moving along an unknown direction with fixed speed that are assumed to be known a priori. Our goal is to detect the motion direction of the unknown target. In the second problem we assume that both the direction and the speed of the targets are unknown. Our objective is to first estimate the speed and use this information to detect the motion direction. We remark that the second problem is biologically realistic but begin our analysis with the first problem because it sheds light on the detectability of B cells in comparison to the A cells. The first problem is also a prerequisite to solving the second.

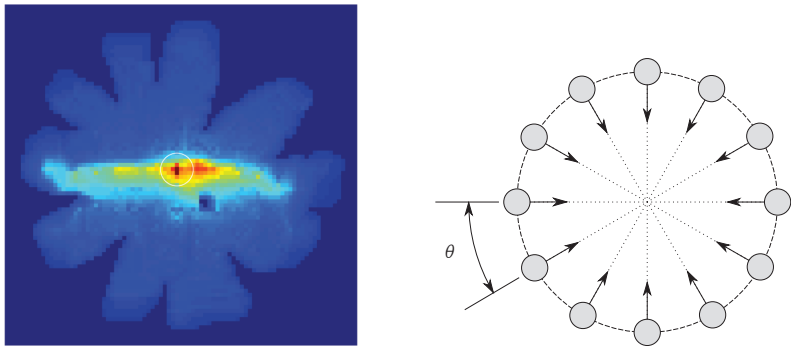

(a) Cells on the turtle retina (b) Paths of the incident light spot

Figure 1: (Left) Distribution of all cells on the retina showing the visual streak. The circle on the center of the streak indicates the location of the retinal patch. (Right) The input to the retina is a circular spot of light moving from one end of the patch to the other in a straight line.

Two methods to detect the unknown motion direction of the target are now described. In the first method, we use Principal Component Analysis (PCA) (see [16], [11]). The spike sequence generated by each cell in the model patch is low pass filtered using a second order linear filter. The filter output is a continuous signal that approximates the spike rate of the corresponding cell in the patch. The vector of spike rate functions over a suitable time window are projected as points on a cartesian coordinate system using PCA. We model these points as realizations of a Gaussian process, conditioned on the direction of motion, and detect the target motion direction using the well known Maximum Likelihood Estimation Method ([22]). In the second method we hypothesize that the pattern of spiking activity in a cell can be described by a class of point process, called Self Exciting Poisson Process (see [20]). We use the fact that a collection of such processes can be pooled together, and under an appropriate hypothesis (see [20]), can be modeled as an inhomogeneous Poisson Process. We

pool together the spiking activities of a subpatch of cells in a patch and represent the pooled activities as an inhomogeneous vector Poisson Process. We estimate intensity functions for each component of this process, conditioned on the input direction of the target. The direction of motion of an unknown input can be detected using estimates of the intensity function vector.

2 Retinal cell modeling and construction of a retinal patch

Turtles, being vertebrates, have a multi layered retinal structure. From the point of view of visual signal processing, it has layers of photoreceptive cells consisting of cones and rods. These cells are synaptic to a layer of ganglion cells which give rise to the optic nerve fibers (see [19]).

We model the layer of photoreceptive cells as a cascade of filters which represent key functions, including the spatial and temporal variation of the receptor field (see [5]) and direction selectivity only for the B cells (see [4]). The ganglion cells are modeled as firing neurons using the Hodgkin-Huxley (HH) model calibrated with parameters from [13] and [14]. Noise is modeled as a zero mean Gaussian current input to the HH model. In the following subsections the function of the major components of the filter model are described. This model was originally reported by Baker [2] and we refer the reader to [7] for details.

The ganglion cells on a turtle retina are distributed in such a way that it is possible to observe a high density of cells along a line called the visual streak. The spatial distribution of turtle ganglion cells on the retina has been studied in [17]. It reports the cell density over a multitude of vertical and horizontal transects as to cover the entire retina. We interpolate the data provided using a two dimensional cubic spline to compute the cell density (both A and B types combined) over the whole retina.

In a subsequent paper [18], the distribution of the size of ganglion cells at some selected sites of the retina has been detailed. By inspecting this data, we can conclude that the histogram of the cell body size is bimodal. We fit this histogram data with sum of two Gaussian distributions. Additionally, we observe from [15], that the A cells have a large soma size compared to B cells. Therefore, we claim that in the bimodal distribution, the A cells are distributed with higher mean cell size and the B cells are distributed with lower mean cell size. The percentage of A cells calculated at each site are interpolated over the entire retina using a two dimensional cubic spline. Multiplying the percentage of A cells with the cell density data calculated as above, we obtain the distribution of A cells over the entire retina. This procedure is repeated for the B cells. Fig. 1a shows the distribution of the entire population of retinal ganglion cells.

Since the turtle retina has 350–390 thousand cells, we use about 1% of that for constructing large-scale models of the full retina. The majority of cells are B cells. The B cells are divided into three equal groups, corresponding to three distinct direction preferences. The A cells are divided in to two equal groups based on their receptor field structure, known as the A-ON and the A-OFF. The three groups of the B cells and the two groups of A cells are randomly sprinkled over the retina to match the computed density functions.

A circular retinal patch has been used to obtain results reported in this paper. The patch is taken to be the cells which are contained in a three millimeter circular disc centered at the location with maximum cell density on the visual streak. It has a total of 520 cells, of which 54 are A-ON cells and 55 are A-OFF cells. The B cell counts are 134, 136 and 141 for the three angle preferences of 180°, 40° and −75° respectively. These are the means of the groups of directional sensitive cells reported in [4].

3 Two simulations using the retinal patch

In this section we detail two different yet related simulations on the model retinal patch. In the first simulation we collect data to determine the unknown motion direction of a point target assuming that the speed of the target is known. In the second simulation we collect data to estimate the speed and use this information to detect motion direction of a point target assuming that both of these parameters are unknown. In both simulations the input is a spot of light on a dark background. The patch is circular of diameter three millimeters and the size of the spot is one tenth the size of the patch.

In Simulation I, we consider a circular retinal patch (shown in Fig. 1a) and assume that a point target moves with a constant velocity through the center of the patch. The target takes 0.8 seconds to cross the patch. The simulation pool consists of motion directions between 0° (i.e. the target moves from left to right) and 358° at steps of 2°. It follows that we have 180 different directions of motion. The objective of this simulation is to study how different cell types discriminate directions of motion. Simulation I is repeated twice, once under the assumption that the B cells have a perfect knowledge of θ. In the second instance, we assume that the B cells are able to observe θ up to a random variable θ^*. Each motion direction is simulated 60 times in the first instance. For the second instance, the directions are simulated 30 times.

In Simulation II, we use twelve different angles from 0° to 330° at steps of 30°. We have the target move along each direction at nine different speeds. As the speed varies, the target takes between 0.4 seconds to 2 seconds to diametrically cross the patch. In all, we have 108 different speed/angle combinations (i.e. 108 different velocities). Each combination is simulated 60 times. In addition to these evenly spaced simulation points, we also generate intermediate test points with five intermediate speeds and 60 intermediate angles. These intermediate points are each simulated 10 times.

4 Two main tools for analysis

The two main tools for analysis we use are derived from the PCA [11] and the Models PPM arising from self exciting point processes [20]. In the Simulation I, the activities of the cells in the patch are low pass filtered individually. The smoothed activity functions are represented using PCA by considering the entire patch as the spatial window and over a suitable sliding time window. The spatiotemporal activity of the retinal patch is thus represented as a strand conditioned on the target direction. Maximum likelihood detection is performed (see Van Trees [22]) assuming that the strand is a Gaussian random process. The details are similar to what had been done by Du et. al. [6] on the turtle visual cortex. Alternatively, in the PPM approach, the spike activities of the cells are pooled over a subpatch and the intensity function of

the pooled process, a Poisson Process, is computed. This step is repeated over a vector of subpatches. The obtained vector of intensity functions is now used to detect the target motion direction.

In the second simulation, the speed of the target is estimated from the intensity function of the pooled spike activities. The pooling process is similar to what was described for the first simulation. The speed estimation is carried out from the *half height pulse widths* of the associated intensity functions. Using the estimated speeds, the target directions are inferred as follows. The intensity functions are first computed over a vector of subpatches and are subsequently rescaled, using the estimated target speeds, to be distributed over an unit length in seconds. The target motion directions are detected from the rescaled intensity functions using PCA over each subpatch. The PCA is carried out over a moving time window and we assume that the principal component points form a Gaussian process. Over every subpatch, target detection is carried out by running a maximum likelihood detection algorithm for Gaussian processes (as performed for data in Simulation I). The final target direction is inferred using a majority vote over the subpatches (see [12, 21]).

5 Results

In addition to providing a model of the A and B cells, one of the main result of this paper is to illustrate the extent to which retinal cells are able to detect direction of target motion. The B cells out-perform the A cells in terms of their ability to discriminate motion direction, measured using Root Mean Square of the detection error. This fact is entirely obvious along the preferred direction of the directionally selective B cells. A priori, it is not clear why an ensemble of three directionally selective families of B cells would have a superior performance for targets moving along any direction. The superiority of the B cell performance over A cell, is particularly enhanced when the target speed is assumed to be unknown. In this case the speed is estimated from the retinal response data. Finally as a population, the B cells out-perform the A cells, even when B cells observe the target direction upto a large noise variance of ($\sim 30^{\circ}$).

For Simulation I, it can be observed from Fig. 2b on the next page that the direction sensitive B cells detect motion directions with less error close to their preferred directions. If we consider the B cells together (shown in Fig. 2a on the next page), then the detection error is constant throughout all the motion angles. A cells, on the other hand, do show a higher level of detection error and some amount of variability with the motion direction. We suspect that this variation is purely due to the distribution of A cells in this specific patch under consideration. In Figs. 3a and 3b on page 121 we plot the Root Mean Square Error using PPM. The displayed results are obtained using a 20 *ms* window and the window starts at 400 *ms*, the mid point of the motion of the target in visual space. Fig. 3a clearly shows the effect of direction sensitive B cells. They out-perform the A cells in terms of having a lower Root Mean Square Error of detection. Also note from Figs. 2a and 3a that, when all three direction preferences of the B cells are taken together, the overall Root Mean Square Error is much lower than any single type and it remains constant over all motion directions.

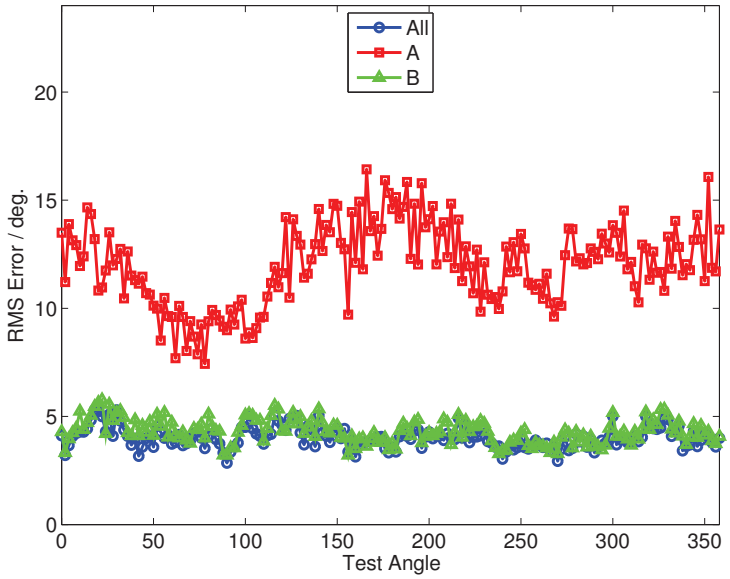

(a) PCA - All cell types

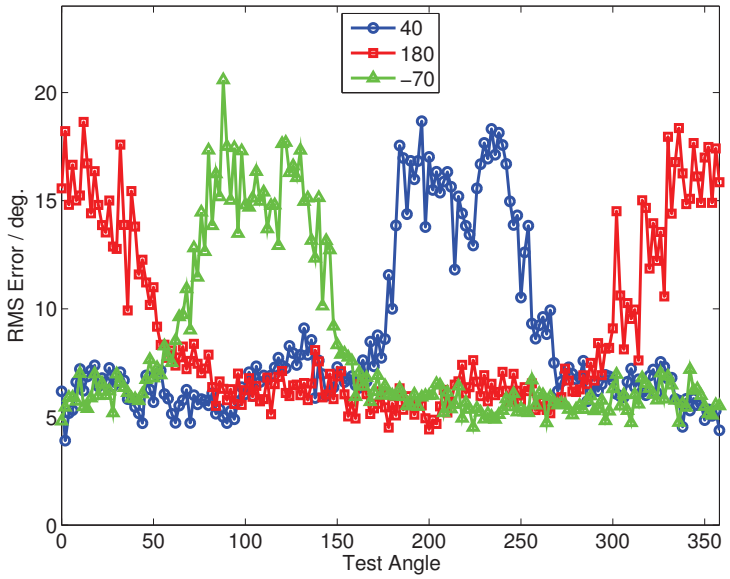

(b) PCA - B cells

Figure 2: Root Mean Square Error of detection using Principal Component Analysis (PCA) for Simulation I.

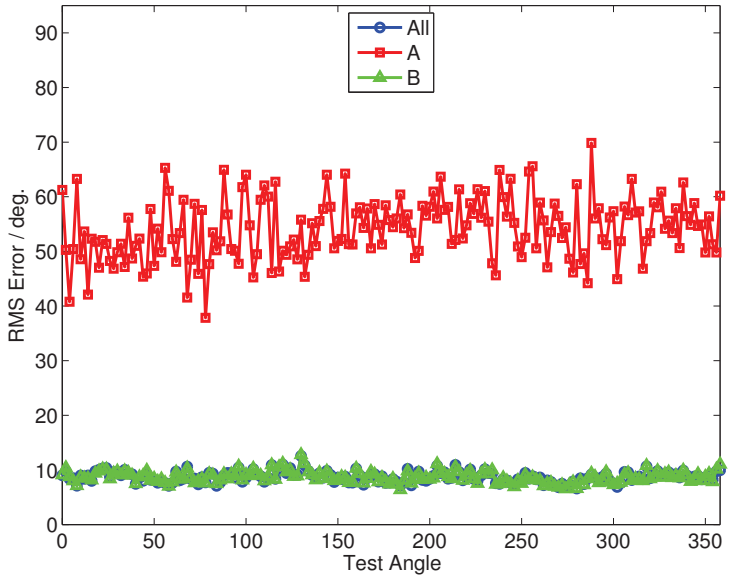

(a) PPM - All cell types

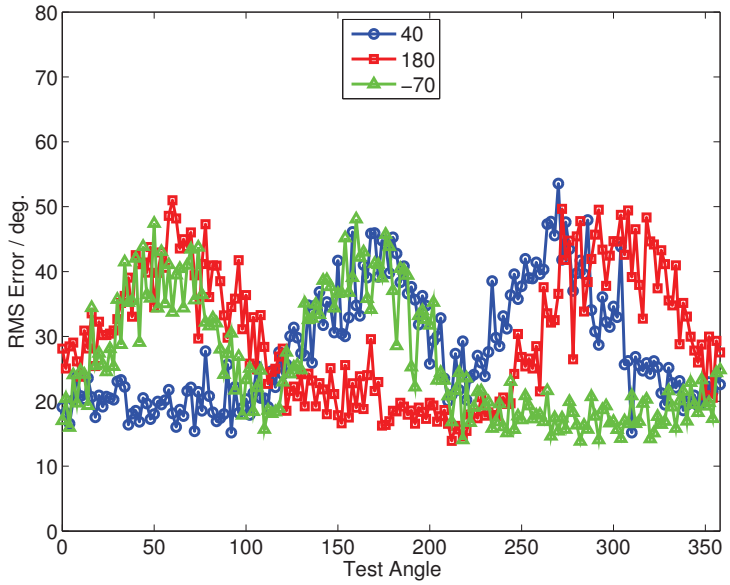

(b) PPM - B cells

Figure 3: Root Mean Square Error of detection using Poisson Process Model (PPM) for Simulation I.

We have omitted (see [7]) discussing the problem of estimating the speed and motion direction using Simulation II. When the speed is unknown and is estimated from the data, the root mean square error for motion direction is larger compared to what is observed in Simulation I. This fact has been illustrated in Figures 4 and 5 where the root mean square error has been plotted as a function of time as the target enters the patch at different speeds.

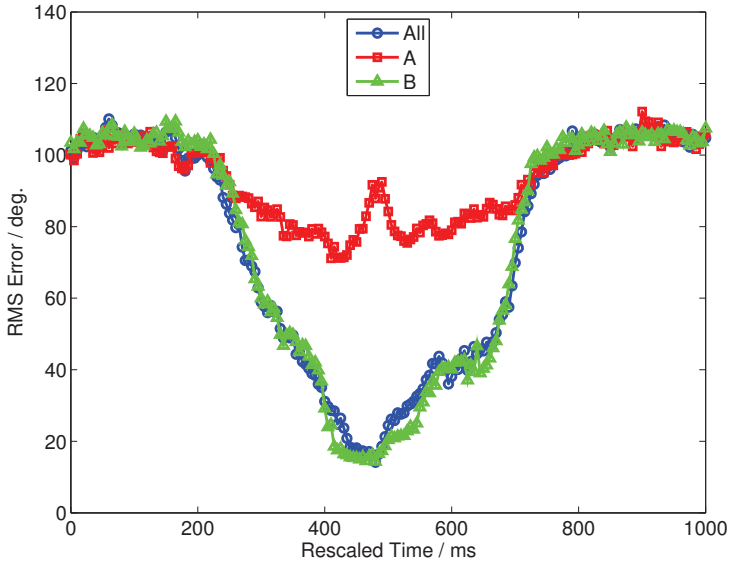

(a) High Speed

Figure 4: For Simulation II variation of the Root Mean Square Error of detection over rescaled time using all cells (blue), A cells (red) and B cells (green). Original *high speed* takes 400 *ms* to cross the patch, *medium speed* and *low speed* are shown in Figure 5.

6 Conclusion

Using Root Mean Square of the detection error as a criterion for measuring detectability, we show in this paper that – for the purpose of discriminating motion directions of targets, the direction-selective B cells are superior compared to the intensity sensitive A cells along their preferred direction, with no particular advantage along the null direction. Taken as a collection, B cells with three specific preferred directions (observed in the turtle retina) have a superior performance compared to the A cells for any target direction. The performance of a *B cell family* remains relatively unaltered under noisy conditions even when individual B cells observe target directions up to a zero mean Gaussian random variable with a large angular variance. All the above properties remain qualitatively intact when the speed of the target is uncertain,

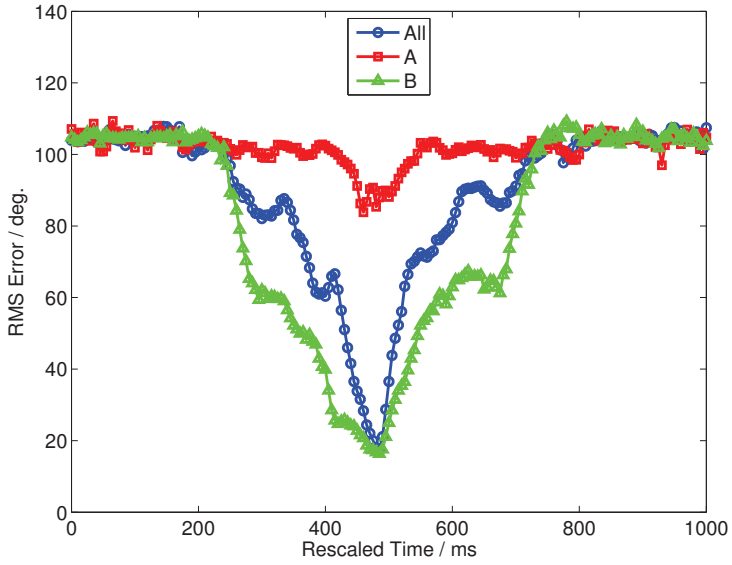

(a) Medium Speed

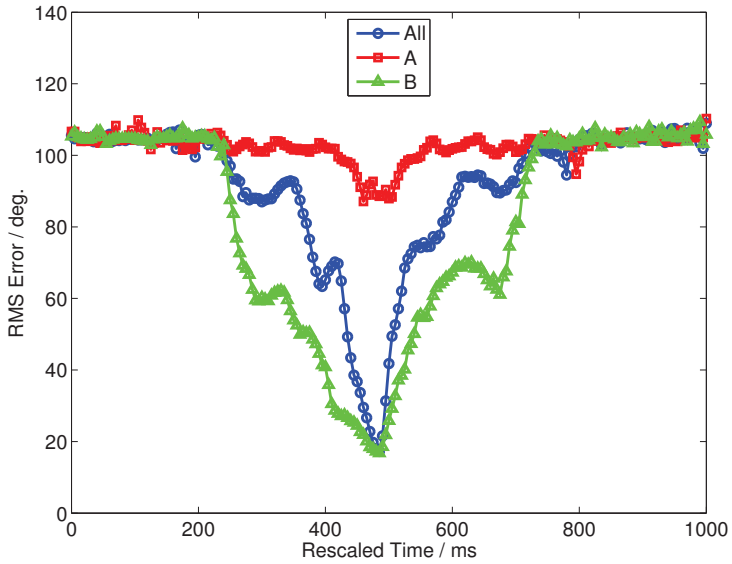

(b) Low Speed

Figure 5: For Simulation II variation of the Root Mean Square Error of detection over rescaled time using all cells (blue), A cells (red) and B cells (green). Original *high speed* (Figure 4) takes 400 *ms*, *medium speed* (top) takes 1200 *ms*, *low speed* (bottom) takes 2000 *ms* to cross the patch.

although the actual values of the RMS errors rise. In this case we show that the RMS error can be decreased by using a voting algorithm that combines detection across multiple subpatches. All the claims made in this paper have been verified using two distinct decoding algorithms – the PCA and PPM.

Acknowledgments

This material is based upon work supported in part by the National Science Foundation under the grant number BIC 0523983 and ECCS 1029178. Any opinions, findings, and conclusions or recommendations expressed in this material are those of the author(s) and do not necessarily reflect the views of the National Science Foundation.

Bibliography

[1] J. Ammermuller and H. Kolb. The organization of the turtle inner retina. I. On and off center pathways. *Journal of Comparative Neurology*, 358(1):1–34, 1995. Cited p. 115.

[2] T. I. Baker and P. S. Ulinski. Models of direction-selective and non-direction selective turtle retinal ganglion cells. *Society for Neuroscience Abstract*, 2001. Cited p. 117.

[3] H. B. Barlow and W. R. Levick. The mechanism of directionally selective units in rabbit's retina. *The Journal of Physiology*, 178:477–504, 1965. Cited p. 115.

[4] D. B. Bowling. Light responses of ganglion cells in the retina of the turtle. *The Journal of Physiology*, 299:173–196, 1980. Cited pp. 115, 117, and 118.

[5] J. R. Dearworth and A. M. Granda. Multiplied functions unify shapes of ganglion-cell receptive fields in retina of turtle. *Journal of Vision*, 2(3):204–217, 2002. Cited p. 117.

[6] X. Du, B. K. Ghosh, and P. S. Ulinski. Encoding and decoding target locations with waves in the turtle visual cortex. *IEEE Transactions in Biomedical Engineering*, 52(4):566–577, 2005. Cited p. 118.

[7] M. P. B. Ekanayake. *Decoding the Speed and Motion Direction of Moving Targets Using a Turtle Retinal Patch Model*. PhD thesis, Texas Tech University, 2011. Cited pp. 116, 117, and 122.

[8] S. Exner. *Entwurf zu einer physiologischen Erklärung der psychischen Erscheinungen, 1. Theil*. F. Deuticke, 1894. Cited p. 115.

[9] A. L. Hodgkin and A. F. Huxley. A quantitative description of membrane current and its application to conduction and excitation in nerve. *The Journal of Physiology*, 117:500–544, 1952. Cited p. 115.

[10] D. H. Hubel. Single unit activity in striate cortex of unrestrained cats. *The Journal of Physiology*, 147:226–238, 1959. Cited p. 115.

[11] I. T. Jolliffe. *Principal Component Analysis*. Springer, 2nd edition, 2002. Cited pp. 116 and 118.

[12] L. Lam and C. Y. Suen. Application of majority voting to pattern recognition: An analysis of its behavior and performance. *IEEE Transactions on Systems, Man and Cybernetics - Part A*, 27(5):553–568, 1997. Cited p. 119.

[13] E. M. Lasater and P. Witkovsky. Membrane currents of spiking cells isolated from turtle retina. *Journal of Comparative Physiology A*, 167(1):11–21, 1990. Cited p. 117.

[14] Y. Liu and E. M. Lasater. Calcium currents in turtle retinal ganglion cells. I. The properties of T- and L-type currents. *Journal of Neurophysiology*, 71(2):733–742, 1994. Cited p. 117.

[15] P. L. Marchiafava and R. Weiler. Intracellular analysis and structural correlates of the organization of inputs to ganglion cells in the retina of the turtle. *Proceedings of the Royal Society of London. Series B, Biological Sciences*, 208(1170):103–113, June 1980. Cited pp. 115 and 117.

[16] Z. Nenadic, B. K. Ghosh, and P. S. Ulinski. Modeling and estimation problems in the turtle visual cortex. *IEEE Transactions in Biomedical Engineering*, 49(8):753–762, 2002. Cited pp. 115 and 116.

[17] E. H. Peterson and P. S. Ulinski. Qunatitative studies of retinal ganglion cells in a turtle, pseudemys scripta elegans I: Number and distribution of ganglion cells. *Journal of Comparative Neurology*, 186:17–42, 1979. Cited p. 117.

[18] E. H. Peterson and P. S. Ulinski. Qunatitative studies of retinal ganglion cells in a turtle, pseudemys scripta elegans II: Size spectrum of ganglion cells and its regional variation. *Journal of Comparative Neurology*, 208:157–168, 1982. Cited pp. 115 and 117.

[19] R. D. Rodieck. *The First Steps in Seeing*. Sinauer, 1998. Cited pp. 115 and 117.

[20] D. L. Snyder. *Random Point Processes*. John Wiley & Sons, 1975. Cited pp. 116 and 118.

[21] S. Theodoridis and K. Koutroumbas. *Pattern Recognition*. Academic Press, 4th edition, 2008. Cited p. 119.

[22] H. L. Van Trees. *Detection, Estimation and Modulation Theory, Part I*. John Wiley & Sons, 1968. Cited pp. 116 and 118.